

Convergence of Eigenvector Continuation

Avik Sarkar^{1,*} and Dean Lee^{1,†}

¹*Facility for Rare Isotope Beams and Department of Physics and Astronomy,
Michigan State University, East Lansing, MI 48824, USA*

Eigenvector continuation is a computational method that finds the extremal eigenvalues and eigenvectors of a Hamiltonian matrix with one or more control parameters. It does this by projection onto a subspace of eigenvectors corresponding to selected training values of the control parameters. The method has proven to be very efficient and accurate for interpolating and extrapolating eigenvectors. However, almost nothing is known about how the method converges, and its rapid convergence properties have remained mysterious. In this letter we present the first study of the convergence of eigenvector continuation. In order to perform the mathematical analysis, we introduce a new variant of eigenvector continuation that we call vector continuation. We first prove that eigenvector continuation and vector continuation have identical convergence properties and then analyze the convergence of vector continuation. Our analysis shows that, in general, eigenvector continuation converges more rapidly than perturbation theory. The faster convergence is achieved by eliminating a phenomenon that we call differential folding, the interference between non-orthogonal vectors appearing at different orders in perturbation theory. From our analysis we can predict how eigenvector continuation converges both inside and outside the radius of convergence of perturbation theory. While eigenvector continuation is a non-perturbative method, we show that its rate of convergence can be deduced from power series expansions of the eigenvectors. Our results also yield new insights into the nature of divergences in perturbation theory.

Eigenvector continuation (EC) is a variational method that finds the extremal eigenvalues and eigenvectors of a Hamiltonian matrix that depends on one or more control parameters [1]. The method consists of projecting the Hamiltonian onto a subspace of basis vectors corresponding to eigenvectors at some chosen training values of the control parameters. It has been used to extend quantum Monte Carlo methods to problems with strong sign oscillations [2], as a fast emulator for quantum many-body systems [3, 4], and as a resummation method for perturbation theory [5]. Eigenvector continuation is well suited for studying the connections between microscopic nuclear forces and nuclear structure, a topic that has generated much recent interest [6–14]. In the future it could be used to study electronic structure as a function of ion positions, geometric phases in the adiabatic evolution of a quantum Hamiltonian, or the quantum phase diagram of a many-body Hamiltonian with several tunable couplings. All of these applications would be greatly enhanced with a better fundamental understanding of the convergence of the method. For that purpose, in this letter we present the first study of the convergence properties of eigenvector continuation.

Let us consider a one-parameter family of Hamiltonian matrices $H(c) = H_0 + cH_1$, where both H_0 and H_1 are finite-dimensional Hermitian matrices. It may be that the Hamiltonian depends on more than one control parameter, but we will restrict to some selected one-parameter family in order to analyze the convergence properties. We are interested in finding the ground state eigenvector $|v(c_t)\rangle$ and eigenvalue $E(c_t)$ for some target parameter value $c = c_t$. The objective of eigenvector continuation is to approximate $|\psi(c_t)\rangle$ as a linear combination of ground state eigenvectors $|v(c_0)\rangle, \dots, |v(c_N)\rangle$ at training points $c = c_0, \dots, c_N$. In eigenvector continuation the best linear combination of training-point vectors is chosen by minimizing the expectation value of $H(c_t)$. As noted in Ref. [1], eigenvector continuation can also be extended to

excited states by including excited state eigenvectors at the training points. However we will focus on ground state calculations in this analysis.

It is convenient to introduce a variant of eigenvector continuation which we will call vector continuation (VC). Like eigenvector continuation, the objective of vector continuation is to approximate $|v(c_t)\rangle$ as a linear combination of vectors $|v(c_0)\rangle, \dots, |v(c_N)\rangle$ at training points $c = c_0, \dots, c_N$. The difference is that in vector continuation we construct the best approximation by projecting $|v(c_t)\rangle$ onto the subspace spanned by the training point vectors. This is a simpler process than the variational calculation used in eigenvector continuation. However it requires knowledge of the target eigenvector and so is not a constructive method for computing $|v(c_t)\rangle$ but, rather, a tool for analyzing the geometry of the eigenvector path $|v(c)\rangle$. In the following we show that eigenvector continuation and vector continuation have nearly identical convergence properties. Therefore it will suffice to understand the convergence properties of vector continuation. As the name suggests, vector continuation can also be generalized to any smooth vector path $|v(c)\rangle$ without reference to Hamiltonian matrices or eigenvectors.

Since we want to understand the convergence of eigenvector and vector continuation at large orders, we consider the case where the sequence of training points c_0, \dots, c_N has some limit point at large N . Without loss of generality we take this limit point to be $c = 0$. In the limit where the training points accumulate around $c = 0$, we can replace our training vectors $|v(c_0)\rangle, \dots, |v(c_N)\rangle$ with the derivatives of $|v(c)\rangle$ at $c = 0$, which we write as $|v^{(0)}(0)\rangle, \dots, |v^{(N)}(0)\rangle$. In the following we write $|v(c_t)\rangle_N^{\text{EC}}$ for the order- N eigenvector continuation approximation to $|v(c_t)\rangle$, and we write $|v(c_t)\rangle_N^{\text{VC}}$ for the order- N vector continuation approximation to $|v(c_t)\rangle$.

Starting from the derivative vectors $|v^{(0)}(0)\rangle, \dots, |v^{(N)}(0)\rangle$, we use Gram-Schmidt orthog-

onalization to define a sequence of orthonormal vectors $|w^{(0)}(0)\rangle, \dots, |w^{(N)}(0)\rangle$. With this orthonormal basis, we can write $|v(c_t)\rangle_N^{\text{VC}}$ as

$$|v(c_t)\rangle_N^{\text{VC}} = \sum_{n=0}^N \langle w^{(n)}(0) | v(c_t) \rangle |w^{(n)}(0)\rangle. \quad (1)$$

Using the same orthonormal basis, we can also write $|v(c_t)\rangle_N^{\text{EC}}$ as

$$|v(c_t)\rangle_N^{\text{EC}} = \sum_{n=0}^N a(c_t, n, N) |w^{(n)}(0)\rangle, \quad (2)$$

where the coefficients $a(c_t, n, N)$ are found by minimizing the expectation value of $H(c_t)$.

We now consider perturbation theory (PT) around the point $c = 0$. If z_0 is the nearest branch point to $c = 0$, then the series expansion

$$|v(c_t)\rangle = \sum_{n=0}^{\infty} |v^{(n)}(0)\rangle \frac{c_t^n}{n!} \quad (3)$$

will converge for $|c_t| < |z_0|$ and diverge for $|c_t| > |z_0|$. We define $|v(c_t)\rangle_N^{\text{PT}}$ as the partial series truncated at order $n = N$,

$$|v(c_t)\rangle_N^{\text{PT}} = \sum_{n=0}^N |v^{(n)}(0)\rangle \frac{c_t^n}{n!}. \quad (4)$$

In this analysis we have assumed that the radius of convergence is greater than zero. This follows from the fact that $H(c)$ is a finite-dimensional Hermitian matrix for all real c . In a forthcoming publication we will discuss the extension to infinite-dimensional systems and the interesting case where the radius of convergence is zero.

We will quantify the error of our three different approximations to $|v(c_t)\rangle$ by computing the norm of the residual vector. In Fig. 1 we plot the logarithm of the error versus order N for eigenvector continuation (asterisks), vector continuation (solid lines), and perturbation theory (dashed lines). The three different colors correspond to three different examples, which we call Models 1A, 1B, and 1C. The Hamiltonians for these three models are given in the Supplemental Materials. We see that in all cases eigenvector continuation and vector continuation converge more rapidly than perturbation theory. Furthermore, we see that eigenvector continuation and vector continuation have nearly identical errors at each order.

Let us now prove that eigenvector continuation and vector continuation indeed have identical convergence properties. We first consider vector continuation at order N . Let $V^N(0)$ be the subspace spanned by $|w^{(0)}(0)\rangle, \dots, |w^{(N)}(0)\rangle$, and let $V_{\perp}^N(0)$ be the orthogonal complement. As one can see from Eq. (1), there is no error at all in the coefficients of $|w^{(0)}(0)\rangle, \dots, |w^{(N)}(0)\rangle$. The residual vector for $|v(c_t)\rangle_N^{\text{VC}}$ lies entirely in $V_{\perp}^N(0)$.

We now consider eigenvector continuation at order N . In this case we project $H(c_t)$ onto $V^N(0)$ and find the resulting

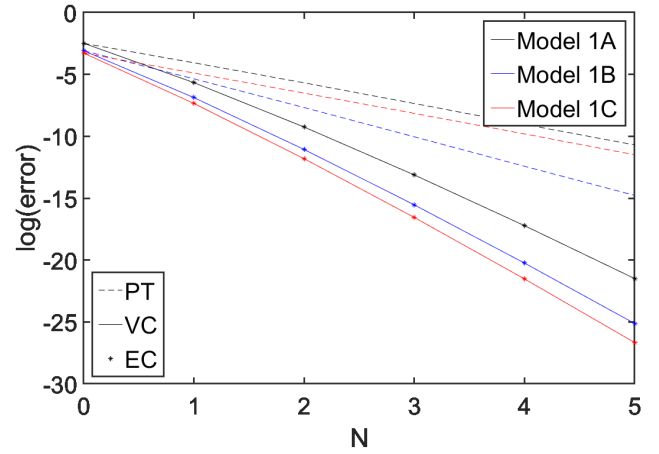


FIG. 1: (Color online) Logarithm of the error versus order N for eigenvector continuation (asterisks), vector continuation (solid lines), and perturbation theory (dashed lines). The three different colors (black, blue and red) correspond with Models 1A, 1B, and 1C respectively.

ground state. In essence, we have turned off all matrix elements of $H(c_t)$ that involve vectors in $V_{\perp}^N(0)$. Let us now turn on these matrix elements as a perturbation. When these matrix elements are turned back on, we will get a first-order correction to the wave function from transition matrix elements connecting $V^N(0)$ with $V_{\perp}^N(0)$. This will produce a correction to the wave function that lies in $V_{\perp}^N(0)$. On the other hand, the corrections to the coefficients of $|w^{(0)}(0)\rangle, \dots, |w^{(N)}(0)\rangle$ will appear at second order in perturbation theory, since this involves pairs of transitions from $V^N(0)$ to $V_{\perp}^N(0)$ and $V_{\perp}^N(0)$ to $V^N(0)$.

Therefore, if the norm of the residual vector for eigenvector continuation is $O(\epsilon)$, then eigenvector continuation and vector continuation will agree at $O(\epsilon^2)$. This proves that eigenvector continuation and vector continuation have identical convergence properties in the limit of large N .

Let us now consider the norm of the “last term” corresponding to $n = N$ in Eqs. (1), (2), and (4),

$$L_N^{\text{VC}}(c_t) = \left| \langle w^{(N)}(0) | v(c_t) \rangle \right|, \quad (5)$$

$$L_N^{\text{EC}}(c_t) = |a(c_t, N, N)|, \quad (6)$$

$$L_N^{\text{PT}}(c_t) = \left\| |v^{(N)}(0)\rangle \frac{c_t^N}{N!} \right\|. \quad (7)$$

Combining Eq. (5) with Eq. (3), we have

$$L_N^{\text{VC}}(c_t) = \left| \sum_{n=N}^{\infty} \langle w^{(N)}(0) | v^{(n)}(0) \rangle \frac{c_t^n}{n!} \right|. \quad (8)$$

In this series expression, we will call the partial series up to $n = N$ the leading order (LO) approximation. We will call the partial series up to $n = N + 1$ the next-to-leading order (NLO) approximation, and so on. The N^k LO approximation

is therefore

$$L_N^{\text{VC}, \text{N}^k \text{LO}}(c_t) = \left| \sum_{n=N}^{N+k} \langle w^{(N)}(0) | v^{(n)}(0) \rangle \frac{c_t^n}{n!} \right|, \quad (9)$$

and at leading order we have

$$L_N^{\text{VC}, \text{LO}}(c_t) = \left| \langle w^{(N)}(0) | v^{(N)}(0) \rangle \frac{c_t^N}{N!} \right|. \quad (10)$$

By comparing Eq. (10) with Eq. (7), we can understand why vector continuation is converging more rapidly than perturbation theory. In general, $|\langle w^{(N)}(0) | v^{(N)}(0) \rangle|$ is smaller than the norm of $|v^{(N)}(0)\rangle$ because $|v^{(N)}(0)\rangle$ is not orthogonal to the lower derivative vectors $|v^{(0)}(0)\rangle, \dots, |v^{(N-1)}(0)\rangle$. Perturbation theory has interference between non-orthogonal terms at different orders, a phenomenon that we call differential folding. Differential folding can be a very large effect, and is the reason why perturbation theory converges more slowly than vector and eigenvector continuation.

In order to study the convergence properties systematically, let us define the convergence ratio obtained by taking two widely separated orders N' and N , with $N > N'$, and computing the quantities

$$\mu^{\text{VC}}(c_t, N, N') = |L_N^{\text{VC}}(c_t)/L_{N'}^{\text{VC}}(c_t)|^{1/(N-N')}, \quad (11)$$

$$\mu^{\text{EC}}(c_t, N, N') = |L_N^{\text{EC}}(c_t)/L_{N'}^{\text{EC}}(c_t)|^{1/(N-N')}, \quad (12)$$

$$\mu^{\text{PT}}(c_t, N, N') = |L_N^{\text{PT}}(c_t)/L_{N'}^{\text{PT}}(c_t)|^{1/(N-N')}. \quad (13)$$

We note that these convergence ratio functions will have cusps where the numerator vanishes and divergences where the denominator vanishes. Fortunately these special points occur at only a few isolated values of c_t , and the functions in Eq. (11), (12), and (13) provide a useful picture of the convergence properties of the three methods. We can eliminate cusps or divergences at any particular value of c_t by changing N or N' .

The convergence ratio for eigenvector continuation, $\mu^{\text{EC}}(c_t, N, N')$, can be calculated directly by using Eq. (6). This is indeed what one should do in practice. In our analysis here, however, we go a step beyond this and predict the convergence ratio entirely from the derivatives of the eigenvectors near $c = 0$. For our discussion of the convergence ratio, we consider an example that we will call Model 2 where perturbation theory will break down due to several avoided level crossings. The details of Model 2 are given in the Supplemental Materials. In Fig. 2 we show the energies of the lowest six energies as a function of the control parameter c . The closest branch point to $c = 0$ occurs very close to the real axis near $c = 0.84$. This can be seen from the avoided level crossing near $c = 0.84$.

In Fig. 3 we show a comparison of the convergence ratios $\mu^{\text{VC}}(c_t, N, N')$, $\mu^{\text{EC}}(c_t, N, N')$, and $\mu^{\text{PT}}(c_t, N, N')$ versus c_t for $N = 20$ and $N' = 0$. We note that in the limit $|N - N'| \rightarrow \infty$, $\mu^{\text{PT}}(c_t, N, N')$ will exceed 1 for $c_t > 0.84$,

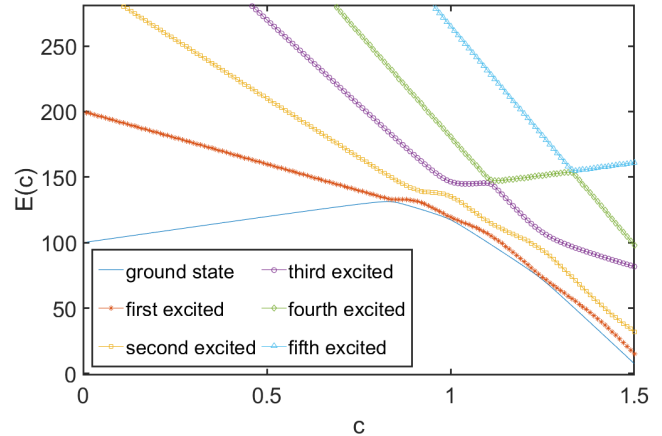


FIG. 2: (Color online) The lowest six energies of Model 2 as a function of c .

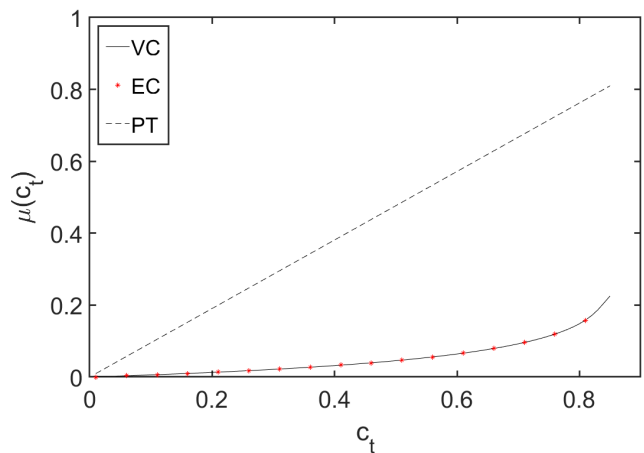


FIG. 3: (Color online) Comparison of the convergence ratios $\mu^{\text{VC}}(c_t, N, N')$, $\mu^{\text{EC}}(c_t, N, N')$, and $\mu^{\text{PT}}(c_t, N, N')$ for Model 2 with $N = 20$ and $N' = 0$.

signalling the divergence of perturbation theory. As shown in Fig. 3, for $N = 20$ and $N' = 0$, the point where $\mu^{\text{PT}}(c_t, N, N')$ crosses 1, is slightly greater than $c_t = 0.84$. On the other hand, $\mu^{\text{VC}}(c_t, N, N')$ and $\mu^{\text{EC}}(c_t, N, N')$ are in close agreement with each other, and remain well below 1 near $c_t = 0.84$.

In Fig. 4 we plot $\mu^{\text{VC}}(c_t, N, N')$ and the LO, NLO, N²LO, and N³LO approximations to $\mu^{\text{VC}}(c_t, N, N')$ for $N = 20$ and $N' = 0$. We see that the series expansion in Eq. (8) converges for c_t within the radius of convergence of perturbation theory, which for this example corresponds to $c = 0.84$. Within the radius of convergence of perturbation theory, we can deduce the convergence ratio of vector continuation from the derivative vectors $|v^{(0)}(0)\rangle, \dots, |v^{(N)}(0)\rangle$. Given the fact that eigenvector continuation and vector continuation have identical convergence ratios in the limit of large $|N - N'|$, this also gives us a good estimate of the convergence ratio for

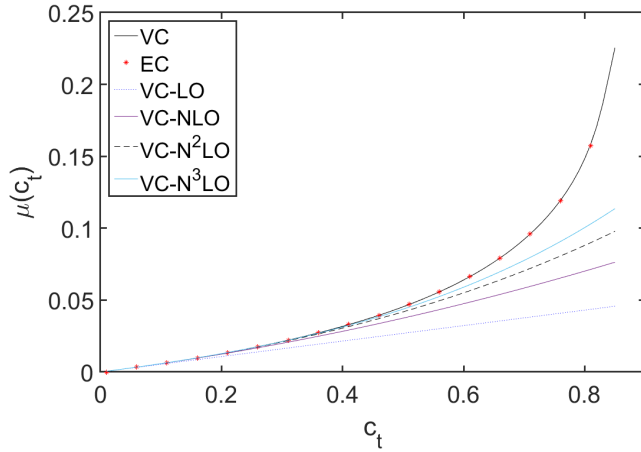


FIG. 4: (Color online) Plots of the convergence ratios $\mu^{\text{VC}}(c_t, N, N')$, $\mu^{\text{EC}}(c_t, N, N')$, and the LO, NLO, N²LO, and N³LO approximations to $\mu^{\text{VC}}(c_t, N, N')$ versus c_t for Model 2 with $N = 20$ and $N' = 0$.

eigenvector continuation.

Outside the radius of convergence of perturbation theory, we can still deduce the convergence ratio from the derivative vectors $|v^{(0)}(0)\rangle, \dots, |v^{(N)}(0)\rangle$ by using extrapolation. If there are no branch points nearby, then the convergence ratio function can be extrapolated using standard methods such as Padé approximants [5] or conformal mapping [15, 16]. In Fig. 5 we plot $\mu^{\text{VC}}(c_t, N, N')$ and $\mu^{\text{EC}}(c_t, N, N')$ for $N = 20$ and $N' = 0$ and negative c_t extending beyond the radius of convergence of perturbation theory. We also show the (1,1) and (2,2) Padé approximants to $\mu^{\text{VC}}(c_t, N, N')$. We see that the Padé approximants describe the shape of $\mu^{\text{VC}}(c_t, N, N')$ quite well since there are no nearby branch points.

If there is a branch point nearby, such as we have for Model 2 near $c = 0.84$, the slope of the convergence ratio function will rise more quickly than predicted by Padé approximants or conformal mapping. This is because at the branch point, the Riemann surface of the ground state eigenvector is entwined with the Riemann surface of the first excited state eigenvector. If the branch point is very close to the real axis, then we have an avoided level crossing or Landau-Zener transition where the wave functions of the ground state and first excited state interchange as we pass by the branch point.

We can therefore predict the rise of $\mu^{\text{VC}}(c_t, N, N')$ and $\mu^{\text{EC}}(c_t, N, N')$ from the fall of $\mu_1^{\text{VC}}(c_t, N, N')$ and $\mu_1^{\text{EC}}(c_t, N, N')$ for the first excited state. We define $\mu_1^{\text{VC}}(c_t, N, N')$ and $\mu_1^{\text{EC}}(c_t, N, N')$ in the same manner as $\mu^{\text{VC}}(c_t, N, N')$ and $\mu^{\text{EC}}(c_t, N, N')$, except that we replace the target ground state $|v(c_t)\rangle$ with the first excited state $|v_1(c_t)\rangle$, while using the same orthonormal basis states $|w^{(n)}(0)\rangle$ associated with the ground state at $c = 0$. For the eigenvector continuation approximation of the first excited state, $|v_1(c_t)\rangle_N^{\text{EC}}$, we use a subspace that includes derivatives of the ground state $|v^{(0)}(0)\rangle, \dots, |v^{(N)}(0)\rangle$ and also derivatives

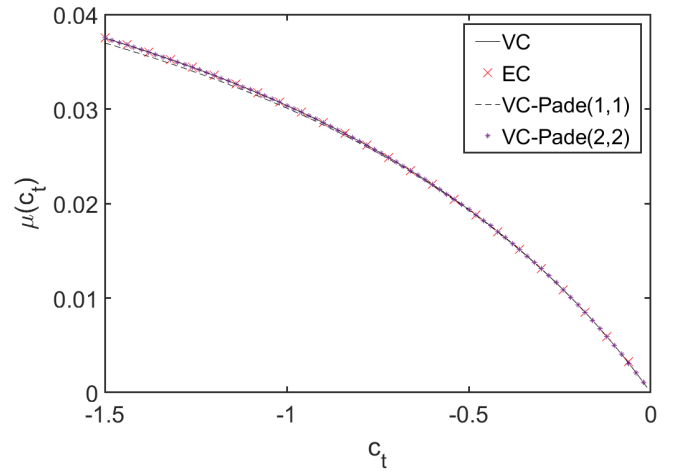


FIG. 5: (Color online) Plots of the convergence ratios $\mu^{\text{VC}}(c_t, N, N')$, $\mu^{\text{EC}}(c_t, N, N')$, and the (1,1) and (2,2) Padé approximants to $\mu^{\text{VC}}(c_t, N, N')$ versus c_t for Model 2 with $N = 20$ and $N' = 0$.

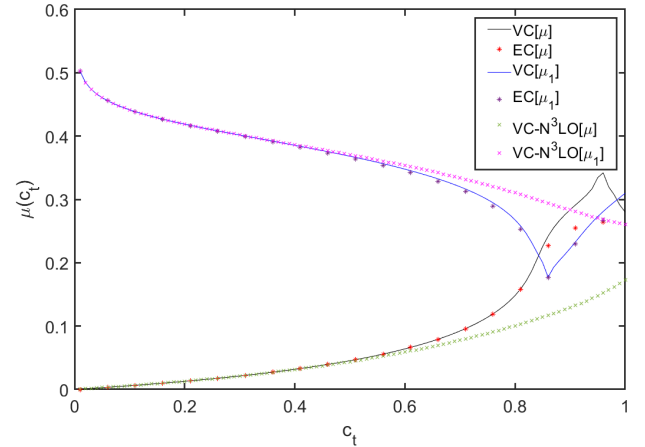


FIG. 6: (Color online) Plots of the convergence ratios $\mu^{\text{VC}}(c_t, N, N')$, $\mu_1^{\text{VC}}(c_t, N, N')$, $\mu^{\text{EC}}(c_t, N, N')$, $\mu_1^{\text{EC}}(c_t, N, N')$, and the N³LO approximations to $\mu^{\text{VC}}(c_t, N, N')$ and $\mu_1^{\text{VC}}(c_t, N, N')$ for Model 2 with $N = 20$ and $N' = 0$.

of the first excited state $|v_1^{(0)}(0)\rangle, \dots, |v_1^{(N)}(0)\rangle$.

In Fig. 6 we show $\mu^{\text{VC}}(c_t, N, N')$, $\mu_1^{\text{VC}}(c_t, N, N')$, $\mu^{\text{EC}}(c_t, N, N')$, $\mu_1^{\text{EC}}(c_t, N, N')$, and the N³LO approximations to $\mu^{\text{VC}}(c_t, N, N')$ and $\mu_1^{\text{VC}}(c_t, N, N')$ for $N = 20$ and $N' = 0$. We note the approximate vertical and horizontal reflection symmetries near the branch point. For $c_t < 0.84$ the increase in the ground-state convergence ratio mirrors the decrease in the excited-state convergence ratio. Also the increase in the ground-state convergence ratio for $c_t > 0.84$ mirrors the decrease in the excited-state convergence ratio for $c_t < 0.84$.

We observe that a great deal of information about the convergence of vector and eigenvector continuation can be pre-

dicted from series expansions around $c = 0$. Near the branch point we know that $\mu^{\text{VC}}(c_t, N, N')$, and therefore also $\mu^{\text{EC}}(c_t, N, N')$, crosses the midpoint of the gap between $N^k\text{LO}$ approximations to $\mu^{\text{VC}}(c_t, N, N')$ and $\mu_1^{\text{VC}}(c_t, N, N')$ for any k . The $N^k\text{LO}$ approximations to $\mu^{\text{VC}}(c_t, N, N')$ and $\mu_1^{\text{VC}}(c_t, N, N')$ are calculated entirely from perturbation theory at $c = 0$. Also, the location of the nearby branch point can itself be deduced from the convergence radius of the series expansion. While there are limits to how far we can go in c_t with these convergence ratio predictions, it is clear that we can predict the convergence ratios both inside and outside the radius of convergence from the derivatives of the eigenvectors near $c = 0$. It is quite intriguing that this information can be used to predict the non-perturbative convergence of vector and eigenvector continuation.

In this letter we have presented the first study of the convergence of eigenvector continuation. We first defined a variant of eigenvector continuation called vector continuation and proved that eigenvector continuation and vector continuation have identical convergence properties. We then observed that the rate of convergence of vector continuation can be deduced from power series expansions of the eigenvectors.

We found that the series expansion of the wave function exhibits an effect called differential folding, the interference among non-orthogonal terms at different orders. Both vector and eigenvector continuation avoid this problem. As a result, they converge faster than perturbation theory and do not diverge for any value of the control parameter. This geometric view of eigenvector continuation is complementary to the analysis based on analytic continuation described in Ref. [1]. While most studies of the divergence of perturbation theory focus on series expansions of energy eigenvalues and other observables [15–21], our results provide new insights into these divergences as arising from large non-orthogonal terms in the series expansion of the wave function.

In our analysis we were able to predict how eigenvector continuation converges outside the radius of convergence of perturbation theory. These findings provide a new understanding of why eigenvector continuation converges so rapidly. As has been observed in numerical applications [3, 4], the fast convergence of eigenvector continuation is particularly striking when interpolating and extrapolating in parameter spaces with many dimensions. All existing and future applications of eigenvector continuation will benefit from this new fundamental understanding of the convergence of the method.

Acknowledgement

We are grateful for discussions with Joey Bonitati, Thomas Duguet, Noam Elkies, Gabriel Given, Caleb Hicks, Sebastian König, Ning Li, Bing-Nan Lu, and Jacob Watkins. We acknowledge partial financial support from the U.S. Department of Energy (DE-SC0018638). The computational resources were provided by Michigan State University, RWTH Aachen University, the Oak Ridge Leadership Computing Fa-

cility, and the Jülich Supercomputing Centre.

* Electronic address: sarkarav@msu.edu

† Electronic address: leed@frib.msu.edu

- [1] D. Frame, R. He, I. Ipsen, D. Lee, D. Lee, and E. Rrapaj, *Phys. Rev. Lett.* **121**, 032501 (2018), 1711.07090.
- [2] D. K. Frame, Ph.D. thesis (2019), 1905.02782.
- [3] S. König, A. Ekström, K. Hebeler, D. Lee, and A. Schwenk (2019), 1909.08446.
- [4] A. Ekström and G. Hagen, *Phys. Rev. Lett.* **123**, 252501 (2019), 1910.02922.
- [5] P. Demol, T. Duguet, A. Ekström, M. Frosini, K. Hebeler, S. König, D. Lee, A. Schwenk, V. Somà, and A. Tichai, *Phys. Rev.* **C101**, 041302(R) (2020), 1911.12578.
- [6] A. Ekström, G. R. Jansen, K. A. Wendt, G. Hagen, T. Papenbrock, B. D. Carlsson, C. Forssén, M. Hjorth-Jensen, P. Navrátil, and W. Nazarewicz, *Phys. Rev.* **C91**, 051301 (2015), 1502.04682.
- [7] S. Elhatisari et al., *Phys. Rev. Lett.* **117**, 132501 (2016), 1602.04539.
- [8] V. Lapoux, V. Somà, C. Barbieri, H. Hergert, J. D. Holt, and S. R. Stroberg, *Phys. Rev. Lett.* **117**, 052501 (2016), 1605.07885.
- [9] M. Piarulli et al., *Phys. Rev. Lett.* **120**, 052503 (2018), 1707.02883.
- [10] B.-N. Lu, N. Li, S. Elhatisari, D. Lee, E. Epelbaum, and U.-G. Meißner, *Phys. Lett.* **B797**, 134863 (2019), 1812.10928.
- [11] S. Binder et al. (LENPIC), *Phys. Rev.* **C98**, 014002 (2018), 1802.08584.
- [12] V. Somà, P. Navrátil, F. Raimondi, C. Barbieri, and T. Duguet, *Phys. Rev.* **C101**, 014318 (2020), 1907.09790.
- [13] S. Gandolfi, D. Lonardoni, A. Lovato, and M. Piarulli (2020), 2001.01374.
- [14] I. Tews, Z. Davoudi, A. Ekström, J. D. Holt, and J. E. Lynn (2020), 2001.03334.
- [15] M. Kompaniets, *J. Phys. Conf. Ser.* **762**, 012075 (2016), 1604.04108.
- [16] K. Van Houcke, F. Werner, and R. Rossi, *Phys. Rev. B* **101**, 045134 (2020), 1911.01345.
- [17] C. M. Bender and T. T. Wu, *Phys. Rev.* **184**, 1231 (1969).
- [18] R. R. Parwani, *Phys. Rev.* **D63**, 054014 (2001), hep-ph/0010234.
- [19] B. Hamprecht and H. Kleinert, *Phys. Lett.* **B564**, 111 (2003), hep-th/0302124.
- [20] P. C. Argyres and M. Unsal, *JHEP* **08**, 063 (2012), 1206.1890.
- [21] A. Cherman, D. Dorigoni, and M. Unsal, *JHEP* **10**, 056 (2015), 1403.1277.

SUPPLEMENTAL MATERIALS

In our example calculations, we used a system of Hamiltonians $H(c) = H_0 + cH_1$, where H_0 and H_1 are Hermitian matrices. In Models 1A, 1B and 1C, we take H_0 to be diagonal matrices, while H_1 is allowed to have diagonal and off-diagonal elements. For all three model calculations, the target value is $c_t = 0.2$.

In Model 1A, we take H_0 to be the matrix with elements $H_0(n, n) = n$ for $n = 1, \dots, 800$. We choose H_1 to be $H_1(n, n) = n$ for $n = 1, \dots, 800$ and

$$H_1(n+2, n) = H_1(n, n+2) = 1, \quad (\text{S1})$$

for $n = 1, \dots, 798$. For this model, the nearest branch point to the origin is located at $c = -0.559 \pm 0.497i$.

In Model 1B, we take H_0 to be the matrix with elements $H_0(n, n) = 2n$ for $n = 1, \dots, 800$. We choose H_1 to be $H_1(n, n) = n$ for $n = 1, \dots, 800$ and

$$H_1(n+2, n) = H_1(n, n+2) = 1, \quad (\text{S2})$$

for $n = 1, \dots, 798$. For this model, the nearest branch point to the origin is located at $c = -1.422 \pm 0.503i$.

In Model 1C, we take H_0 to be the matrix with elements $H_0(n, n) = 100n$ for $n = 1, \dots, 800$. We choose H_1 to be $H_1(1, 1) = -100$, $H_1(2, 2) = -200$, $H_1(n, n) = -75n$ for $n = 3, \dots, 800$, and

$$H_1(n+1, n) = H_1(n, n+1) = 1, \quad (\text{S3})$$

for $n = 1, \dots, 799$. For this model, the nearest branch point to the origin is located at $c = 0.907 \pm 0.255i$.

In Model 2 we take H_0 to be a 500×500 diagonal matrix with entries $H_0(n, n) = 100n$ for $n = 1, \dots, 500$. H_1 is a 500×500 matrix with nonzero entries as follows:

$$H_1(1, 1) = 40, \quad (\text{S4})$$

$$H_1(2, 2) = -80, \quad (\text{S5})$$

$$H_1(3, 3) = -180, \quad (\text{S6})$$

$$H_1(4, 4) = -260, \quad (\text{S7})$$

$$H_1(5, 5) = -320, \quad (\text{S8})$$

$$H_1(6, 6) = -335, \quad (\text{S9})$$

for $n = 6, \dots, 499$:

$$H_1(n+1, n) = H_1(n, n+1) = 2, \quad (\text{S10})$$

for $n = 6, \dots, 498$:

$$H_1(n+2, n) = H_1(n, n+2) = 5, \quad (\text{S11})$$

for $n = 6, \dots, 497$:

$$H_1(n+3, n) = H_1(n, n+3) = 5, \quad (\text{S12})$$

for $n = 6, \dots, 500$:

$$H_1(n, n) = 50n. \quad (\text{S13})$$

For Model 2, the nearest branch point to the origin is located at $c = 0.840 \pm 0.018i$.